Asian Journal of Chemistry; Vol. 29, No. 9 (2017), 1933-1940

ASIAN JOURNAL OF CHEMISTRY

https://doi.org/10.14233/ajchem.2017.20617

Factors Affecting the Process of Anodic Dissolution Under Electropolishing Conditions by Adsorption of Polymers Molecules on Carbon Steel Surface

HAMDY F.M. EL-SHAMY[1], Y.A. AGGOUR[1], A.M. AHMED[2] and MERVETTE EL-BATOUTI[2]

[1]Department of Chemistry, Faculty of Science, Damietta University, Damietta, Egypt
[2]Department of Chemistry, Faculty of Science, Alexandria University, Alexandria, Egypt

*Corresponding author: E-mail: hamdi.alex88@yahoo.com

Received: 1 March 2017; *Accepted*: 19 May 2017; *Published online*: 15 July 2017; AJC-18469

Many corrosion inhibitors can be used to eliminate the undesirable destructive effect and prevent carbon steel dissolution. Polymers were found to inhibit the process of anodic dissolution. It is found that the limiting current of anodic dissolution decreases with increasing concentration of the natural polymers (*viz.*, starch, chitosan, cellulose acetate and carboxymethyl cellulose sodium salt) which indicated the increase in inhibition efficiency and the stabilization of passive layer of polymers molecules as protective film on carbon steel surface. The effect of viscosity of the solution at different concentrations and temperatures were studied. Dissolution rate and percentage inhibition was determined by weight loss method. Values of activation energy indicate that the rate controlled step is the diffusion of aqueous species in the boundary layer and the isokinetic temperatures were estimated. Those polymers verify Flory-Huggins isotherm. Negative values of free energy of adsorption revealing to the spontaneous adsorption of polymers molecules on carbon steel surface. The adsorption of these polymers molecules on the anode surface was confirmed by scanning electron microscopy. Forced convection mechanism were applied and we obtained that the flow in system were turbulent flow.

Keywords: Natural polymers, Anodic dissolution, Inhibition efficiency, Passive layer.

INTRODUCTION

The mechanism of anodic corrosion is usually explained by its effect occurs because of differential dissolution, as the current is applied and the oxidization film covering the lower peaks of the surface [1]. Elmore was studied the current-voltage relationship for the polishing of copper in orthophosphoric acid system. He attributed the polishing effect to a varying concentration gradient of the dissolved metal ions over the protrusions and valleys [2,3].

Mass-transport limitations for the anode are commonly believed to be responsible for anodic corrosion and this theory is supported by the observation in many experimental systems of polishing for anodic dissolution with a limiting-current plateau [4-8].

According to the wide range applications of carbon steel [9-13], several methods have been applied to reduce the corrosion and make up passive layer, which act as protective film on its surface. The use of inhibitors is one of the most practical methods for the protection against corrosion in acidic media.

To be effective, an inhibitor must also displace the water from the metal surface, interact with anodic or cathodic reaction sites to retard the oxidation and reduction corrosion reaction and prevent transportation of water and corrosion on active species to the surface [14].

The inhibiting action of these natural polymers is usually attributed to their interaction with carbon steel surface *via* their adsorption. Polar functional groups are regarded as the reaction center that stabilizes the adsorption process. In general, the adsorption of inhibitor on metal surface depends on the nature and the surface charge of the metal, the adsorption mode, its chemical structure and the type of electrolyte solution [8].

The aim of the present work is to study the effect of natural polymers namely starch, chitosan, cellulose acetate and carboxymethyl cellulose sodium salt on the rate of anodic corrosion of carbon steel and to make stabilization of a secrified protective film on its surface.

This work were supported with using scanning electron microscope (SEM) examination of surface morphology of carbon steel. The data obtained were ensured the experimental measurements. Dissolution rate and percentage inhibition were measured by weight loss method. Changes in temperature, concentration of inhibitors, type of cell and physical properties of solution such as density and viscosity are studied. Dimensionless analysis investigations used to correlated among all

these parameters. Adsorption isotherm and isokinetic temperatures were simulated.

EXPERIMENTAL

The electrolyte was prepared by using 8 M AnalaR grade H_3PO_4 (98 % w/w), supplied by Sigma-Aldrich Chemicals Ltd. The solution used in cell consist of 8 M H_3PO_4 and different concentrations from the polymers in the range of concentration (100-800 ppm) were used.

As shown in Fig. 1, the electrodes were rectangular carbon steel sheets of 10 cm height and 5 cm width, Luggin tube filled with phosphoric acid was acted as a reference electrode. A porous PVC diaphragm was used in case of divided cell.The active surface of the anode was 3 cm height and another parts of it were insulated with polystyrene lacquers.The rate of anodic dissolution was measured as the limiting current that obtained from polarization curves [15]. A driven carbon steel metal cylinder shaft anode with 1 cm diameter and 3 cm length was used in case of forced convection mechanism.

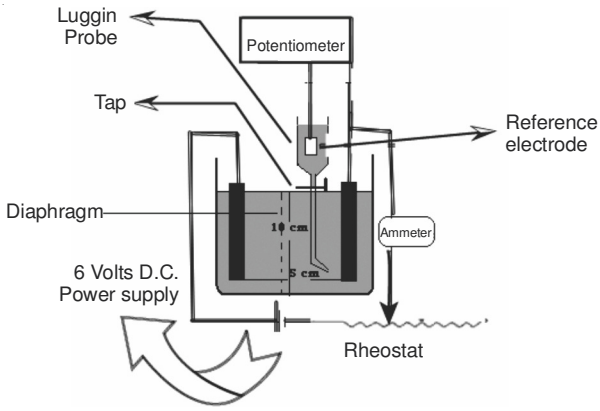

Fig. 1. Cell and 6 V D.C. power supply electrical circuit

Weight loss method: Analytical balance was used to weight a carbon steel coupon had a rectangular form with dimensions (length 5 cm), width (1 cm) and thickness (0.025 cm) before and after immersing in100 mL of aerated 8 M H_3PO_4 solution containing the polymers at the desired concentration for 3 days at 25 °C. In each run the coupons were polished, washed with distilled water, degreased with ethanol and dried at room temperature [16].

Density and viscosity measurements: An Ubelhode type viscometer is used for measurement of the viscosity of the solutions used. The density was determined by using DA-300 Kyoto Electronics at 25, 30, 35 and 40 °C. Density and viscosity measurements were carried out in a circulating ultra thermostat mode (MWL type U 10) where the temperature is adjusted to an accuracy of ± 0.05 °C. The values of densities and viscosities of 8 M phosphoric acid and different polymers-water-phosphoric acid mixtures which were used in the process of dissution were measured at different concentrations.

Scanning electron microscope (SEM) examination: The electron source was LAB6 Electron detection was carried out with a scintillation photodetector. The typical working pressure was 8 mbar and dimensional of (1 cm × 1 cm) carbon steel sheet anodes were used [17]. Before the SEM observation, each electrode was first rinsed with distilled water and with analytical grade acetone. The surface morphology of carbon steel samples immersed in acidic bath (H_3PO_4) with or without polymers additives has studied**.** All experiments were made when the limiting current obtained for all solutions at 25 °C, 8 M H_3PO_4.

RESULTS AND DISCUSSION

Anodic dissolution of carbon steel: Many mechanisms have been proposed successively for the process of anodic dissolution: Salt film (dissolution products) mechanism, acceptor mechanism, preferential adsorption of shielding molecules [18,19] and formation of solid oxide film for aluminum.

The rate of anodic dissolution was represented by the limiting current, which was observed from current-voltage polarization curves. Fig. 2 shown an elevation on rate of anodic dissolution with rising the experimental temperature.

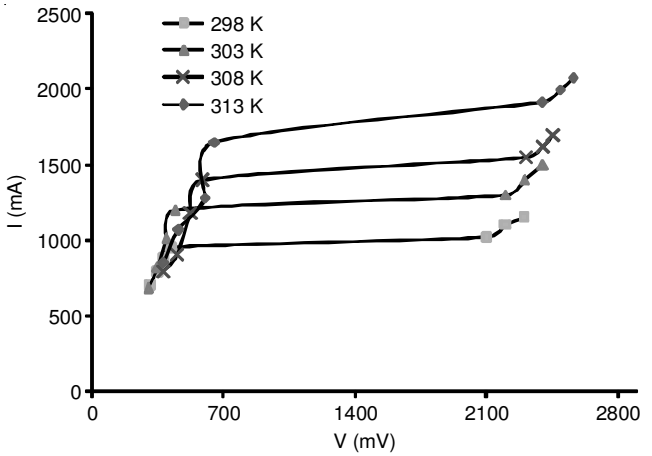

Fig. 2. Relation between current (I) and potential (V) for 8 M H_3PO_4 at 3 cm anode height and different temperatures

Concentration of corrosion inhibitors: The stabilization of passive layer of polymers molecules as protective film on carbon steel surface was ensured by the result that shown in Table-1. The limiting current of anodic dissolution decreases with increasing concentration of the polymers which indicated the increase in inhibition efficiency according to the equation:

$$\text{Inhibition } (\%) = (I\text{-}I^{o}/I) \times 100 \quad (1)$$

where I is limiting current without inhibitor, I^{o} is limiting current with inhibitor.

It is indicated that when raising the temperature the limiting current increases, due to the catalytic effect of anodic dissolution process.

Cell with diaphragm *versus* cell without diaphragm: A porous PVC diaphragm was used to make the division of the cell. Table-1 showed the comparison between the limiting current measured using divided and undivided cell at the same temperatures.

As shown in Fig. 3, divided cell (using a diaphragm) had been reduced the anodic limiting current. A diaphragm had been prevented the uprising hydrogen bubbles that induce a radial momentum transfer. So that the rate of anodic dissolution on carbon steel surface was decreased in case of divided cell which make support to the stabilization of passive layer of polymers as a corrosion inhibitors on carbon steel surface [20].

TABLE-1
VALUES OF LIMITING CURRENT (I_L) AT DIFFERENT TEMPERATURES FOR 8 M H_3PO_4, 3 cm HEIGHT AT DIFFERENT CONCENTRATIONS OF POLYMERS IN CASE OF USING UNDIVIDED CELL AND DIVIDED CELL

Natural polymers additives	Conc. (ppm)	Cell without diaphragm				Cell with diaphragm			
		25 °C	30 °C	35 °C	40 °C	25 °C	30 °C	35 °C	40 °C
Starch	0.00	1020	1300	1550	1920	800	1050	1250	1600
	100	885	1150	1400	1750	730	920	1180	1450
	200	850	1050	1300	1650	680	870	1080	1400
	300	780	1000	1200	1550	630	800	980	1350
	400	700	900	1100	1450	560	750	850	1250
	500	660	870	1000	1300	500	700	800	1150
	600	600	800	900	1200	450	600	700	1050
	700	580	750	850	1150	400	550	650	950
	800	550	700	800	1100	350	490	600	850
Cellulose acetate	0.00	1020	1300	1550	1920	800	1050	1250	1600
	100	750	950	1150	1500	550	800	900	1200
	200	700	900	1100	1400	510	750	880	1150
	300	650	840	980	1300	480	640	800	1050
	400	600	780	900	1200	450	580	700	1000
	500	560	700	850	1100	380	500	620	950
	600	500	620	750	1000	300	450	500	850
	700	440	580	680	900	250	400	450	780
	800	400	500	650	860	210	350	400	680
Carboxymethyl cellulose sodium salt (CMC)	0.00	1020	1300	1550	1920	800	1050	1250	1600
	100	790	1020	1200	1570	600	820	950	1280
	200	750	950	1150	1480	580	780	890	1200
	300	680	850	1000	1380	530	660	840	1100
	400	640	800	950	1230	480	600	740	1050
	500	575	750	900	1140	390	545	660	1000
	600	520	640	780	1020	310	500	580	920
	700	460	580	700	930	270	480	520	830
	800	410	550	680	900	230	440	540	710
Chitosan	0.00	1020	1300	1550	1920	800	1050	1250	1600
	100	810	1050	1250	1600	640	850	1000	1300
	200	760	980	1190	1480	600	800	900	1200
	300	690	880	1050	1400	550	680	850	1150
	400	645	820	990	1240	490	600	750	1100
	500	585	700	880	1150	400	550	670	1060
	600	530	650	790	1050	320	510	590	940
	700	480	600	740	950	280	480	500	850
	800	440	570	700	920	240	380	450	750

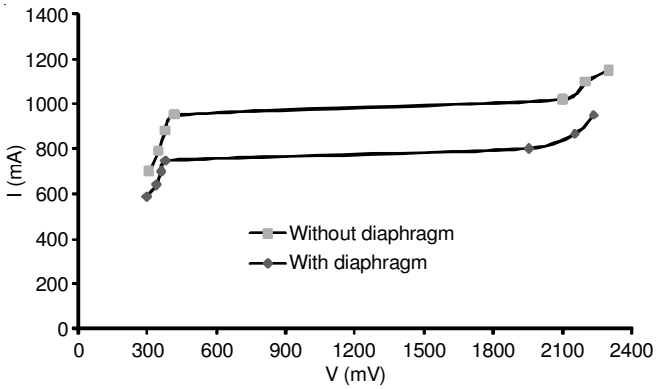

Fig. 3. Limiting current with and without diaphragm for blank solution at 298 K

Effect of solution on viscosities: The motions of the molecules and the movement of one layer of molecules with respect to another layer are responsible for viscous solution [21]. These motions had been illustrated as transitional and rotational motions. The effect of raising the temperature on the viscosity can be tested by the Arrhenius relationship [22].

$$\eta = Ae^{E/RT} \quad (2)$$

where, E is the activation energy of the flow of the polymer molecules to surpass the energy barrier, T is the temperature and R is the molar gas constant.

It was found that as the viscosity increase, the mobility of the polymer molecules in the examined solution have been decreased. Decreasing the mobility retard the rate of anodic dissolution. As shown in Table-2, the viscosity increase by the increasing the concentration of solution containing polymers molecules and decreased by increasing temperature.

Kinematic viscosity (ν) that used to get the diffusion coefficient (D), of Fe^{2+} ions in solutions containing polymers molecules can be calculated from the following equation [20]:

$$\nu = \eta/\rho \quad (3)$$

where η is the viscosity in g $cm^{-1}s^{-1}$ and ρ is the density in g cm^{-3}. It is noted that (1 poise = 1 g $cm^{-1}s^{-1}$) so (1 centipoise = 0.01 g $cm^{-1}s^{-1}$).

Flory-Hugins adsorption isotherm: Reactions in electrochemistry have been suggested by using the application of adsorption isotherm. Flory-Huggins, Langmuir, Bockris-

TABLE-2
VALUES OF VISCOSITIES (centipoise) AND DENSITIES (g cm^{-3}) OF THE DIFFERENT MIXTURES OF NATURAL POLYMERS WITH H_3PO_4 AT DIFFERENT TEMPERATURES

Natural polymers additives	Conc. (ppm)	25 °C		30 °C		35 °C		40 °C	
		ρ	η	ρ	η	ρ	η	ρ	η
Starch	0.00	1.395	1.75	1.350	1.62	1.304	1.50	1.245	1.38
	100	1.205	2.05	1.170	1.93	1.125	1.80	1.101	1.74
	200	1.197	2.06	1.162	1.94	1.123	1.82	1.106	1.77
	300	1.195	2.08	1.160	1.95	1.121	1.85	1.104	1.80
	400	1.193	2.10	1.158	1.97	1.107	1.86	1.109	1.81
	500	1.214	2.15	1.138	1.98	1.105	1.88	1.103	1.82
	600	1.225	2.18	1.142	2.01	1.122	1.92	1.088	1.84
	700	1.219	2.22	1.146	2.04	1.127	1.95	1.101	1.87
	800	1.216	2.25	1.155	2.08	1.131	1.98	1.104	1.90
Cellulose acetate	0.00	1.395	1.75	1.350	1.62	1.304	1.50	1.245	1.38
	100	1.309	2.75	1.268	2.60	1.241	2.47	1.220	2.38
	200	1.308	2.80	1.288	2.68	1.238	2.50	1.207	2.39
	300	1.298	2.83	1.286	2.70	1.244	2.55	1.220	2.44
	400	1.309	2.88	1.282	2.73	1.240	2.58	1.222	2.48
	500	1.295	2.90	1.273	2.75	1.238	2.60	1.229	2.52
	600	1.296	2.93	1.274	2.79	1.224	2.62	1.226	2.55
	700	1.307	2.98	1.279	2.84	1.212	2.63	1.212	2.57
	800	1.326	3.05	1.271	2.86	1.205	2.65	1.205	2.59
Carboxymethyl cellulose sodium salt (CMC)	0.00	1.395	1.75	1.350	1.62	1.304	1.50	1.245	1.38
	100	1.378	2.62	1.351	2.50	1.322	2.38	1.320	2.31
	200	1.380	2.65	1.365	2.54	1.324	2.41	1.316	2.33
	300	1.392	2.70	1.362	2.56	1.321	2.43	1.317	2.37
	400	1.374	2.72	1.353	2.57	1.335	2.47	1.319	2.40
	500	1.382	2.75	1.354	2.60	1.337	2.50	1.315	2.42
	600	1.386	2.80	1.355	2.63	1.333	2.52	1.317	2.45
	700	1.389	2.82	1.352	2.65	1.330	2.54	1.319	2.48
	800	1.390	2.85	1.353	2.68	1.325	2.57	1.321	2.51
Chitosan	0.00	1.395	1.75	1.350	1.62	1.304	1.50	1.245	1.38
	100	1.351	2.50	1.311	2.36	1.268	2.22	1.264	2.15
	200	1.356	2.55	1.311	2.40	1.264	2.25	1.262	2.17
	300	1.358	2.58	1.313	2.43	1.255	2.26	1.259	2.19
	400	1.347	2.60	1.317	2.45	1.258	2.29	1.261	2.22
	500	1.354	2.64	1.319	2.48	1.261	2.32	1.264	2.25
	600	1.363	2.70	1.302	2.50	1.257	2.35	1.254	2.27
	700	1.365	2.73	1.291	2.53	1.247	2.37	1.257	2.30
	800	1.361	2.75	1.288	2.55	1.250	2.40	1.259	2.33

Swinkels, Temkin, Frumkin relations are generally used to calculate the isotherms [23].

The adsorption mechanism of formation and stabilize of a protective layer on the carbon steel were estimated form of these isotherms which have the general form:

$$f(x,\theta)\, e^{(-a\theta)} = KC \quad (4)$$

where f (θ, x) is the configuration factor which depends essentially on the physical and assumptions underlying the derivation of the isotherm [24].

The degree of surface coverage θ at constant temperature was determined from this equation:

$$\theta = I\text{-}I^{o}/I \quad (5)$$

where I is limiting current without inhibitor, I^o is limiting current with inhibitor.

Flory-Huggins adsorption isotherm for carbon steel anode in H_3PO_4 solution, plotted as log θ/C against log (1-θ) at 25 °C. The experimental data fit the Flory-Huggins adsorption isotherm, which is represented by [25]:

$$\log \theta/C = \log xK + x \log (1-\theta) \quad (6)$$

where x is the number of water molecules replaced by one molecule of the inhibitor. The calculated values of X and K are given in Table-3.

TABLE-3
VALUES OF FREE ENERGY OF ADSORPTION (kJ mol^{-1}) AND THE VALUES OF K AND X OF PHOSPHORIC ACID IN PRESENCE OF DIFFERENT POLYMERS USING FLORY-HUGGINS ADSORPTION ISOTHERM

Polymers additives	Flory-Huggins					
	Cell without diaphragm			Cell with diaphragm		
	X	K	$-\Delta G_{ads}$ (KJ mol^{-1})	X	K	$-\Delta G_{ads}$ (KJ mol^{-1})
Starch	1.235	1.001	9.95	0.373	2.814	12.45
Cellulose acetate	1.639	1.813	11.42	0.873	2.904	12.59
CMC	1.333	1.608	11.13	0.639	2.835	12.53
Chitosan	1.442	1.462	10.89	0.511	2.989	12.66

The adsorption of inhibitors at metal-solution interface may be due to the formation of electrostatic or covalent bonding between the adsorbents and the metal surface [26].

Adsorption free energy (ΔG_{ads}) at different concentration was calculating from the following equation [25,27]:

$$\Delta G_{ads} = -RT \ln (55.5\ K) \quad (7)$$

where, T is the experimental temperature in Kelvin (298 K), R is the molar gas constant (8.314 J. K^{-1}.mol^{-1}) and value (55.5) is the concentration of water in the solution mol/L [25,26].

Adsorption free energy in case of cell with and without diaphragm are given in Table-3. It is found that all values are negative which indicate that the adsorption of the inhibitor occur spontaneously and more positive than -40 KJ/mol indicating that the inhibitors are physically adsorbed on the metal surface [28]. The values lie in the range of 9.95-11.42 KJ/mol for cell without diaphragm and 12.54-12.66 KJ/mol for cell with diaphragm. These results indicate that the cell with diaphragm has higher efficiency for adsorption of polymers molecules than the cell without diaphragm because it has higher negatively values of adsorption free energy. The stability of a passive layers of polymers on carbon steel surface was found in the following order:

Cellulose acetate > Carboxymethyl cellulose sodium salt (CMC) > Chitosan > Starch

SEM micrographs of carbon steel: Scanning electron microscope (SEM) examination of anodic corrosion of metals has widely studied [29,30]. This is important to indicate if these inhibitors are efficient or not by study the behaviour of polymers molecules on carbon steel surface.

The SEM analysis (Fig. 4a) shows the morphology of carbon steel as a row material. The surface is rough and uneven surface and large number of pits with large size and high depth distributed over the surface are seen (Fig. 4b) shows the morphology of carbon steel in blank solution, Only a slight difference in the surface morphology was observed in which cavities and small pits are represented clearly.

Fig. 4c and 4f show slightly roughness and more homogenous surface. Deep cavities are eliminated by filling up, also, grain boundaries are decreased gradually. This behaviour may be due to involvement of starch and chitosan molecules in the cavities of steel surface so appear more uniform than blank. According to Fig. 4d and 4e the metallic surface seems to be uniform, smooth, bright and almost not affected by corrosion. Morphology in micrograph (Fig. 4g) appear uniform, smooth and bright more than Fig. 4c. This seems to be due to adsorption of starch increases because of the increase in concentration.

Fig. 4h show the SEM micrograph for steel surfaces at the higher temperatures (45 °C) it shows uniform, smooth and bright surface to some extent more than at lower temperature (25 °C).

It is found that the presence of polymers molecules make a passive layer act as protective film on carbon steel surface and improve the surface morphology on it. So these polymers act as a good corrosion inhibitors.

Isokinetic temperatures relationships: Thermodynamic treatment and activation energy were studied [31-33] and the data has been obtained as shown in Table-4. Energy of activation ΔG^* can be obtained by the equation:

$$\Delta G^* = \Delta H^* - T\Delta S^* \quad (8)$$

The changes in either, or both, the enthalpy or the entropy make change in the rate within a reaction series. The correlation between ΔH^* and ΔS^* is a linear relationship may given as:

$$\delta\Delta H^* = \beta\Delta S^* \quad (9)$$

The operator, δ, concerns difference between any two reactions in series. Substituting from the eqn. 8, we obtain:

$$\beta\delta\Delta S^* = \delta\Delta G^* + T\delta\Delta S^* \quad (10)$$

It is follows that when $\delta\Delta G^*$ = zero, then β = T. In other words, the slope in a linear plot of ΔH^* *versus* ΔS^* is the temperature at which all reactions that conform to the line occur at the same rate. β is therefore known as the isokinetic temperature.

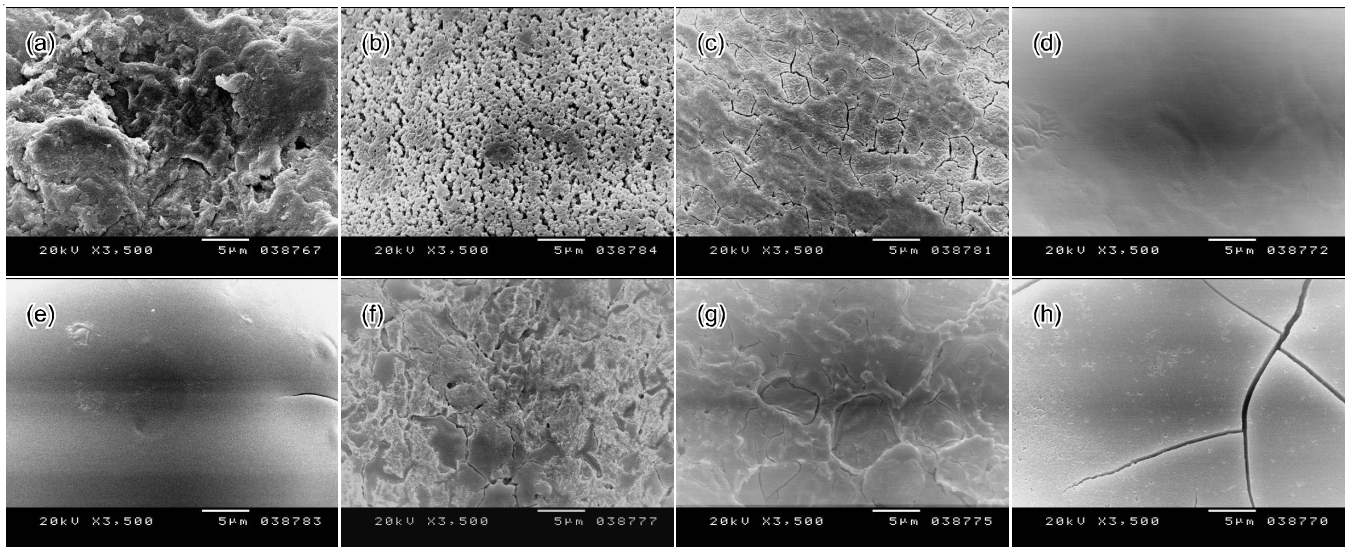

Fig. 4. SEM micrographs for carbon steel surfaces in precence and absence of polymers additives [(a) raw material, (b) after EP (blank), (c) after EP 400 ppm starch, (d) after EP 400 ppm cellulose acetate, (e) after EP 400 ppm CMC, (f) after EP 400 ppm chitosan, (g) after EP 800 ppm starch, (h) after EP at high temperature starch

TABLE-4
VALUES OF THERMODYNAMIC PARAMETERS AT 298 K FOR 8 M H_3PO_4, 3 cm HEIGHT AT DIFFERENT CONCENTRATIONS OF NATURAL POLYMERS IN CASE OF USING CELL WITH AND WITHOUT DIAPHRAGM

Natural polymers additives	Conc. (ppm)	Cell without diaphragm				Cell with diaphragm			
		E_a (kJ mol^{-1})	ΔH^* (kJ mol^{-1})	$-\Delta S^*$ (J mol^{-1} K^{-1})	$-\Delta G^*$ (kJ mol^{-1})	E_a (kJ mol^{-1})	ΔH^* (kJ mol^{-1})	$-\Delta S^*$ (J mol^{-1} K^{-1})	$-\Delta G^*$ (kJ mol^{-1})
Starch	0.00	32.17	29.69	86.85	55.57	34.96	32.48	79.53	56.18
	100	34.80	32.32	79.20	55.9	35.78	33.30	77.62	56.43
	200	34.14	31.66	81.94	56.08	36.95	34.47	74.29	56.61
	300	34.78	32.30	80.45	56.28	38.53	36.05	69.72	56.83
	400	36.97	34.49	73.96	56.53	39.24	36.76	68.22	57.09
	500	33.71	31.23	85.27	56.64	40.77	38.29	63.90	57.33
	600	34.05	31.57	84.93	56.88	41.73	39.25	61.74	57.65
	700	33.88	31.40	85.85	56.98	42.80	40.32	59.08	57.93
	800	34.28	31.80	85.02	57.14	44.40	41.92	54.76	58.24
Cellulose acetate	0.00	32.17	29.69	86.85	55.57	34.96	32.48	79.53	56.18
	100	35.18	32.70	79.45	56.38	38.14	35.66	71.72	57.03
	200	35.36	32.88	79.36	56.53	40.36	37.88	64.90	57.22
	300	34.61	32.13	82.52	56.72	39.86	37.38	67.39	57.46
	400	34.44	31.96	83.69	56.90	40.03	37.55	67.48	57.66
	500	34.39	31.91	84.52	57.10	45.87	43.39	49.43	58.12
	600	35.15	32.67	83.02	57.41	50.01	47.53	37.21	58.62
	700	35.72	33.24	81.94	57.66	54.73	52.25	22.83	59.05
	800	39.67	37.19	69.72	57.97	56.71	54.23	17.51	59.45
Carboxymethyl cellulose sodium salt (CMC)	0.00	32.17	29.69	86.85	55.57	34.96	32.48	79.53	56.18
	100	34.48	32.00	81.28	56.22	37.55	35.07	73.21	56.89
	200	34.58	32.10	81.44	56.37	35.87	33.39	79.12	56.97
	300	35.40	32.92	79.61	56.65	37.67	35.19	74.04	57.26
	400	33.06	30.58	87.93	56.78	39.57	37.09	68.64	57.55
	500	34.70	32.22	83.11	56.99	46.74	44.26	46.11	58.00
	600	34.34	31.86	85.35	57.30	52.92	50.44	26.99	58.48
	700	35.63	33.15	82.02	57.59	53.53	51.05	25.74	58.72
	800	39.86	37.38	68.64	57.84	55.78	53.30	19.17	59.01
Chitosan	0.00	32.17	29.69	86.85	55.57	34.96	32.48	79.53	56.18
	100	34.39	31.91	81.36	56.16	35.52	33.04	79.45	56.72
	200	34.07	31.59	82.94	56.31	34.05	31.57	84.93	56.88
	300	35.59	33.11	78.78	56.59	37.69	35.21	73.71	57.18
	400	33.35	30.87	86.68	56.70	40.99	38.51	63.73	57.50
	500	34.90	32.42	82.61	57.04	48.34	45.86	40.62	57.97
	600	34.75	32.27	83.85	57.26	52.41	49.93	28.40	58.39
	700	34.97	32.49	83.85	57.48	52.28	49.80	29.81	58.68
	800	37.45	34.97	76.21	57.68	55.58	53.10	20.34	59.16

The isokinetic plot of ΔH^* and ΔS^* for different concentrations of the polymers under study.

The temperature less than 298 K indicate that the rate of the reaction is entropy control (starch) in case of cell without diaphragm which is greater than 298 K indicate enthalpy control reaction (cellulose acetate, CMC and chitosan in case of cell without diaphragm and all compounds in case of cell with diaphragm) [31].

Estimation of percentage inhibition of different polymers using weight loss method: The free dissolution of carbon steel in 8 M H_3PO_4 in the presence and absence of polymers were used followed by measuring the loss in weight at 25 °C. From weight loss data, the corrosion rate (g m^{-2} h^{-1}) was calculated for different concentrations of the polymers. Loss in weight per area cm^2 (w_t) can be calculated from the following relation:

$$W_t = \frac{W_0 - W_1}{A} \quad (11)$$

where W_0 is the original weight (mg) of carbon steel specimen. W_1 is the weight after immersion in test electrolyte and A is the surface area in cm^2.

The corrosion rate (CR) can be calculated from the following equation:

$$CR = \frac{W_o - W_1}{A_t} \quad (12)$$

where t is the immersion time in(day).

The percentage inhibition efficiency (IE %) over the exposure time was calculated according to the following equations:

$$IE\,(\%) = \frac{CR_{un} - CR_{in}}{CR_{un}} \quad (13)$$

where CR_{un} and CR_{in} are the corrosion rate (mg m^{-2} day^{-1}) without and with the inhibitor, respectively [34]. The results indicated that the percentage inhibition efficiency of polymers on carbon steel surface was founded in the following order:

Cellulose acetate > Carboxymethyl cellulose sodium salt (CMC) > Chitosan > Starch

Table-5 shows the values of the percentage inhibition efficiency and the corrosion rate obtained from weight loss measurements of carbon steel in presence of different concentrations of the used polymers in 8 M H_3PO_4 solution.

TABLE-5
VALUES FOR NATURAL POLYMERS ADDITIVES

Conc. (ppm)	Weight (g)		Weight loss (g)	Corrosion rate (g m^{-2} h^{-1})	Inhibition (%)	Weight (g)		Weight loss (g)	Corrosion rate (g m^{-2} h^{-1})	Inhibition (%)
	Before	After				Before	After			
	Starch					Cellulose acetate				
100	6.157	6.15254	0.00446	1.22142	12.38	5.422	5.41343	0.00857	1.06209	23.81
200	5.557	5.55083	0.00617	1.15507	17.14	6.882	6.87171	0.01029	0.99573	28.57
300	6.529	6.52043	0.00857	1.06209	23.81	5.556	5.54194	0.01406	0.84964	39.05
400	5.652	5.64171	0.01029	0.99573	28.57	5.592	5.57589	0.01611	0.77005	44.76
500	6.457	6.44500	0.01200	0.92938	33.33	6.548	6.52914	0.01886	0.66382	52.38
600	6.780	6.76457	0.01543	0.79653	42.86	5.686	5.66543	0.02057	0.59747	57.14
700	6.582	6.56486	0.01714	0.73018	47.62	6.706	6.68372	0.02228	0.53111	61.90
800	6.498	6.47880	0.01920	0.65058	53.33	6.248	6.22400	0.02400	0.46462	66.67
	CMC					Chitosan				
100	5.981	5.97236	0.00864	1.05944	24.0	5.428	5.42114	0.00686	1.12844	19.05
200	5.757	5.74663	0.01037	0.99253	28.8	6.056	6.04743	0.00857	1.06209	23.81
300	5.393	5.38119	0.01181	0.93677	32.8	5.652	5.63931	0.01269	0.90275	35.24
400	5.711	5.69631	0.01469	0.82525	40.8	5.315	5.29957	0.01543	0.79653	42.86
500	6.410	6.39301	0.01699	0.73603	47.2	6.793	6.77586	0.01714	0.73018	47.62
600	6.721	6.70170	0.01930	0.64682	53.6	6.929	6.91049	0.01851	0.67707	51.43
700	5.629	5.60682	0.02218	0.53530	61.6	6.655	6.63546	0.01954	0.63734	54.28
800	5.689	5.66567	0.02333	0.49069	64.8	6.545	6.52203	0.02297	0.50449	63.81

These Tables show that an increase in the inhibitor concentration results in an increase of the inhibition efficiency in phosphoric acid solution and this can be attributed to the adsorption of the inhibitors on the carbon steel surface [34].

Inhibition efficiency increases with increasing the immersion time. This indicates that the stabilization of passive film by adsorption of polymers molecules as protective film formed on carbon steel surface in the presence of these inhibitors [35].

Forced convection mechanism: Forced convection mechanism were applied using rotating carbon steel cylinder the results indicates that the anodic dissolution process of carbon steel is diffusion controlled reaction [36,37]. The dimensionless groups Sherwood (Sh), Renold (Re) Schmidt (Sc) were calculated. The data can be correlated by:

Starch $Sh = 0.2891\ Re^{0.715}\ Sc^{0.33}$

Cellulose acetate $Sh = 0.3041 Re^{0.711} Sc^{0.33}$

CMC $Sh = 0.2999 Re^{0.712}\ Sc^{0.33}$

Chitosan $Sh = 0.2951\ Re^{0.714}\ Sc^{0.33}$

The exponent of Renold were found nearly about (0.7) which indicates that the flow in system were turbulent flow and mechanism of the system were forced convection mechanism.

Conclusion

The rate of anodic dissolution on carbon steel surface was decreased in case of increasing concentration of the polymers and using a cell with diaphragm which make support to the stabilization of passive layer of polymers as a corrosion inhibitors on carbon steel surface.

It was observed an elevation on rate of anodic dissolution with rising the experimental temperature. Due to the catalytic effect of anodic dissolution process, viscosity increases by increasing the concentration of solution containing polymers molecules and decreased by increasing temperature. Free energy that obtained from Flory-Hugins adsorption isotherm indicate that the adsorption of the inhibitor occur spontaneously and the values were more positive than -40 KJ/mol indicating that the inhibitors are physically adsorbed on the metal surface.

SEM micrograph for steel surfaces show that the presence of polymers molecules make a passive layer act as protective film on carbon steel surface and improve the surface morphology on it. So these polymers act as a good corrosion inhibitors.

Isokinetic relationship indicated that the rate of the reaction is entropy control for starch in case of cell without diaphragm. And enthalpy control reaction for (cellulose acetate, CMC and chitosan) in case of cell without diaphragm and all polymers that used in case of cell with diaphragm.

The percentage inhibition efficiency of polymers on carbon steel surface was found in the following order:

Cellulose acetate > Carboxymethyl cellulose sodium salt (CMC) > Chitosan > Starch

Forced convection mechanisms were applied and we obtained that the flow in system were turbulent flow.

REFERENCES

1. M. Inman, E. Taylor and T. Hall, *J. Electrochem. Soc.*, **160**, E94 (2013); https://doi.org/10.1149/2.044309jes.
2. D. Gonnella, R. Eichhorn, F. Furuta, M. Ge, D. Hall, V. Ho, G. Hoffstaetter, M. Liepe, T. O'Connell, S. Posen, P. Quigley, J. Sears, V. Veshcherevich, A. Grassellino, A. Romanenko and D.A. Sergatskov, *J. Appl. Phys.*, **117**, 023908 (2015); https://doi.org/10.1063/1.4905681.
3. E.M. Sherif and S.M. Park, *J. Electrochem. Soc.*, **152**, B428 (2005); https://doi.org/10.1149/1.2018254.
4. E.-S.M. Sherif, *Surf. Sci. Appl.*, **252**, 8615 (2006); https://doi.org/10.1016/j.apsusc.2005.11.082.
5. N. Lezi and A. Economou, *Electroanalysis*, **27**, 2313 (2015); https://doi.org/10.1002/elan.201500127.
6. P. Kanyong, G. Hughes, R.M. Pemberton, S.K. Jackson and J.P. Hart, *Anal. Lett.*, **49**, 236 (2016); https://doi.org/10.1080/00032719.2015.1070166.
7. M. Scendo, D. Poddebnia and J. Malyszko, *J. Appl. Electrochem.*, **33**, 287 (2003); https://doi.org/10.1023/A:1024117230591.
8. El-Sayed M. Sherif, A.M. El Shamy, M.M. Ramla and A.O.H. El-Nazhawy, *Mater. Chem. Phys*., **102**, 231 (2007); https://doi.org/10.1016/j.matchemphys.2006.12.009.
9. A.H. Mahmoudi, A. Ghasemi, G.H. Farrahi and K. Sherafatnia, *Mater. Des.*, **90**, 478 (2016); https://doi.org/10.1016/j.matdes.2015.10.162.

10. J.-E. Qu, X. Guo and Z. Chen, *Mater. Chem. Phys.*, **93**, 388 (2005); https://doi.org/10.1016/j.matchemphys.2005.03.028.
11. N. Bellakhal and M. Dachraoui, *Mater. Chem. Phys.*, **85**, 366 (2004); https://doi.org/10.1016/j.matchemphys.2004.01.011.
12. T. Hryniewicz and K. Rokosz, *Front. Mater.*, **1**, 3 (2014); https://doi.org/10.3389/fmats.2014.00003.
13. Y. Wang, E. Laborda and R.G. Compton, *J. Electroanal. Chem.*, **670**, 56 (2012); https://doi.org/10.1016/j.jelechem.2012.02.016.
14. T. Poornima, J. Nayak and A.N. Shetty, *Corros. Sci.*, **53**, 3688 (2011); https://doi.org/10.1016/j.corsci.2011.07.014.
15. K.C. Honeychurch, J. Brooks and J.P. Hart, *Talanta*, **147**, 510 (2016); https://doi.org/10.1016/j.talanta.2015.10.032.
16. T. Asai, T. Konishi and Y. Sasaki, *J. Chem. Eng. Jpn*, **21**, 107 (1988); https://doi.org/10.1252/jcej.21.107.
17. M. Arvand, N. Ghodsi and M.A. Zanjanchi, *Biosens. Bioelectron.*, **77**, 837 (2016); https://doi.org/10.1016/j.bios.2015.10.055.
18. Y. Teng, W. Liu, M. Lan, S. Ma and C. Ma, *Anal. Lett.*, **49**, 299 (2016); https://doi.org/10.1080/00032719.2015.1070164.
19. A. Noor, *Mater. Chem. Phys.*, **114**, 533 (2009); https://doi.org/10.1016/j.matchemphys.2008.09.065.
20. S.M.H. Gangaraj, M. Guagliano and G.H. Farrahi, *Surf. Coat. Technol.*, **243**, 39 (2014); https://doi.org/10.1016/j.surfcoat.2012.03.057.
21. M.C. Ross, Proceedings of SRF2015, Whistler, BC, Canada, p. MOBA01 (2015).
22. S. Arrhenius, *Z. Physik Chem.*, **1**, 285 (1887); https://doi.org/10.1515/zpch-1887-0133.
23. C. Kokkinos, M. Prodromidis, A. Economou, P. Petrou and S. Kakabakos, *Electrochem. Commun.*, **60**, 47 (2015); https://doi.org/10.1016/j.elecom.2015.08.006.
24. U. Ateya, B.E. El-Anadouli and F.M. El-Nizamy, *Corros. Sci.*, **24**, 509 (1984); https://doi.org/10.1016/0010-938X(84)90033-7.
25. H. Otmacic and E. Stupnisek-Lisac, *Electrochim. Acta*, **48**, 985 (2003); https://doi.org/10.1016/S0013-4686(02)00811-3.
26. E.E. Ebenso, *Bull. Electrochem.*, **19**, 209 (2003).
27. E.E. Ebenso and P. Cokafor, *Bull. Electrochem.*, **17**, 459 (2001).
28. R.D. Kaushik, R.R. Malik, J. Singh and Manila, *Int. J. Chemtech Res.*, **6**, 3122 (2014).
29. A.-M.M. Ahmed, A.A.-H. Abdel-Rahman and A.F. El Adl, *J. Dispers. Sci. Technol.*, **31**, 343 (2010); https://doi.org/10.1080/01932690903192598.
30. T. Juuti, S. Uusikallio, A.J. Kaijalainen, E. Heinonen, N.T. Tun and D.A. Porter, *Mater. Sci. Forum*, **879**, 873 (2016); https://doi.org/10.4028/www.scientific.net/MSF.879.873.
31. M. El-Batouti, S.H. Salaam, A.M. Ahmed and H.F.M. El-Shamy, *Asian J. Chem.*, **28**, 965 (2016); https://doi.org/10.14233/ajchem.2016.19450.
32. H. Ashassi-Sorkhabi, B. Shaabani and D. Seifzadeh, *Appl. Surf. Sci.*, **239**, 154 (2005); https://doi.org/10.1016/j.apsusc.2004.05.143.
33. M. Bouklah, N. Benchat, A. Aouniti, B. Hammouti, M. Benkaddour, M. Lagrenée, H. Vezin and F. Bentiss, *Prog. Org. Coat.*, **51**, 118 (2004); https://doi.org/10.1016/j.porgcoat.2004.06.005.
34. S.M. Dinnappa and R.K. Mayanna, *J. Appl. Electrochem.*, **11**, 111 (1981); https://doi.org/10.1007/BF00615329.
35. D. Mohamed, A. Keera and S. Farid, *Egypt J. Petrol.*, **13**, 87 (2004).
36. H.H. Abdel-Rahman and M.A. Darweesh, *Egypt. J. Chem.*, **49**, 19 (2006).
37. N.M. El-Mallah, A.M. Ahmed and L.F. Gado, *J. Dispers. Sci. Technol.*, **31**, 1579 (2010); https://doi.org/10.1080/01932690903218005.